Diffusion MR Imaging During Acute Subarachnoid Hemorrhage in Rats

Elmar Busch, Christian Beaulieu, Alex de Crespigny and Michael E. Moseley

Stroke. 1998;29:2155-2161
doi: 10.1161/01.STR.29.10.2155
Stroke is published by the American Heart Association, 7272 Greenville Avenue, Dallas, TX 75231

Print ISSN: 0039-2499. Online ISSN: 1524-4628

Diffusion MR Imaging During Acute Subarachnoid Hemorrhage in Rats

Elmar Busch, MD; Christian Beaulieu, PhD; Alex de Crespigny, PhD; Michael E. Moseley, PhD

Background and Purpose—We analyzed the temporal and spatial pattern of water diffusion changes during acute subarachnoid hemorrhage (SAH) in rat brain to identify factors contributing to the acute pathophysiology of SAH.

Methods—Subarachnoid hemorrhage was remotely induced via perforation of the circle of Willis with an endovascular suture during MR imaging. A fast echo-planar imaging technique was used to acquire 60 maps of the apparent diffusion coefficient (ADC) beginning 1 min before and continuing for 11 min after induction of SAH. A high-resolution spin-echo diffusion sequence was used to follow diffusion changes over 6 h after SAH. Sham-operated control (n=3), nonheparinized (n=6), and heparinized (n=5) groups were studied.

Results—Sham-operated control animals did not show ADC changes over time. In both SAH groups, however, a sharp decline of ADC within 2 min of SAH was consistently observed in the ipsilateral somatosensory cortex. These decreases in diffusion then spread within minutes over the ipsilateral hemisphere. Similar ADC decreases on the contralateral side started with a further time delay of 1 to 3 min. From 30 min onward, the extent of the diffusion abnormality decreased progressively in the nonheparinized animals. No recovery was observed in heparinized rats.

Conclusions—MR diffusion imaging allows new insight into the pathophysiology of acute SAH: The spatial and temporal pattern of diffusion changes suggests the initial occurrence of acute vasospasm and subsequently "spreading depolarization" of brain tissue. Persistent hemorrhage in heparinized animals was reflected by early decline of ADC values throughout the entire brain. **(*Stroke*. 1998;29:2155-2161.)**

Key Words: magnetic resonance imaging ■ spreading cortical depression ■ subarachnoid hemorrhage ■ vasospasm ■ rats

The pathophysiology of acute subarachnoid hemorrhage (SAH) in humans is poorly understood because it is difficult to study systematically. Until now, the sequence of events leading to the early deterioration and death of patients with SAH has remained unknown. With the prospect of an increasing number of treatment options for acute cerebral ischemia, detailed knowledge of the pathophysiology of acute SAH becomes more important.[1–3]

Animal studies focusing on the early time course of SAH have made progress in closely simulating human SAH.[4,5] Many of these studies found a sudden and transient decrease of cranial perfusion pressure (CPP) resulting from an increase in intracranial pressure (ICP). Because changes in cerebral blood flow (CBF) did not always parallel changes in CPP, it was suggested that early vasospasm might play an additional role in these experimental settings.[4,6,7] However, the impact of these events on acute and chronic brain metabolism is unknown.[8]

MR diffusion-weighted imaging (DWI) is a powerful tool for the noninvasive detection of early brain injury.[9,10] The sharp decline of the apparent diffusion coefficient (ADC) of water after cerebral ischemia is related to cellular swelling due to cell depolarization, and it can occur as early as 2 minutes after onset of ischemia.[11,12] Using fast imaging techniques, brain water diffusion changes can be monitored with high temporal and spatial resolution and therefore might allow more detailed insight into the pathophysiology of acute SAH.

See Editorial Comment, page 2161

The purpose of this study was to test whether the acute events during SAH cause transient or permanent changes in brain water diffusion in a rat model. Furthermore, we aimed to identify factors contributing to the acute pathophysiology of SAH, eg, vasospasm, by analyzing the spatial and temporal pattern of possible DWI changes.

One group of animals was pretreated with heparin in order to prevent blood clotting and thereby increase the severity of the induced hemorrhage. By comparing the heparin-treated rats with those not given heparin, we could test whether the temporal and spatial pattern of DWI changes is related to the severity of the hemorrhage. This aspect is of particular importance if DWI would be used to monitor the impact of acute SAH in patients.

Materials and Methods

Surgical Procedures and Physiological Monitoring

All animal procedures were approved by the Stanford Animal Care Committee. Fourteen Sprague-Dawley rats weighing 290 to 370 g were

Received May 27, 1998; final revision received June 26, 1998; accepted June 29, 1998.

From the Department of Radiology, Stanford University, Stanford, Calif (C.B., A. d C., M.E.M.), and Neurologische Universitaetsklinik, Essen, Germany (E.B.).

Correspondence to Dr Elmar Busch, Neurologie, Universitaetsklinikum Essen, Hufelandstr 55, D-45122 Essen, Germany. E-mail elmar.busch@uni-essen.de

anesthetized with 3% halothane in air, supplemented with O_2. Halothane levels were later reduced to a maintenance dose of 1% to 1.5%. The rats were intubated and ventilated, and the femoral artery and vein were cannulated for continuous monitoring of blood pressure, withdrawal of blood samples, and administration of fluid and drugs.

SAH was induced within the magnet by perforation of the circle of Willis via an endovascular monofilament.[4,13] In brief, the right carotid artery was dissected and the CCA and pterygopalatine artery ligated. The ECA was intersected and its stump placed in line with the ICA. Thirty-five millimeters of a 3.0 prolene suture was connected to a PE 90 tube and positioned inside a guide sheath (PE 260), the tip of which was fixed next to the carotid bifurcation at the digastric muscle.[13] The suture was introduced through the ECA stump into the ICA. The ECA was tightened around the suture to prevent blood loss and fixed at the tip of the guide sheath. The tip of the suture was positioned at the level of the skull base. The animal was positioned on its back, fixed in a stereotactic head holder, and placed inside the magnet. After localizer MRI scans and control images were acquired, SAH was induced without moving the animal by advancing the suture a further 16 mm, followed by immediate withdrawal to its position at the skull base. The procedure of advancing and withdrawing the suture inside the magnet took less than 30 s. In control animals, the thread was advanced only a further 11 mm, followed by immediate withdrawal, so that its tip reached the MCA origin but did not perforate the circle of Willis.[13]

At hourly intervals arterial blood samples were taken for measurement of blood gases (Blood Gas System 288, Ciba Corning Diagnostics), and ventilation parameters were adjusted to keep the blood gases in physiological range. Body temperature was recorded with a rectal thermometer and maintained at 37°C with a forced warm air supply. Blood pressure was measured continuously via a transducer and recorded on a computerized data acquisition system (MacLab, ADInstruments Inc).

Experimental Protocol

Three groups were studied: control animals (n=3), nonheparinized animals with SAH (n=6), and heparinized animals with SAH (n=5). Control and nonheparinized animals were observed with MRI as described below for 6 h. At 6 h, the animals were killed with an intravenous injection of potassium chloride, and the brains were inspected and processed for 2,3,5-triphenyltetrazolium chloride (TTC) staining. Heparinized animals received 50 IU heparin after surgery and again immediately before SAH to prevent blood clotting. In the latter group, MR studies were continued for 2 h after SAH (only 2 h because the rats were brain dead by this point), after which the brains were examined.

Inspection of Brains and TTC Staining

At the end of the observation period, the brains were visually inspected through the surgical microscope (magnification, ×2) for the presence of SAH and photographically documented. Afterward, the brains were incubated for 10 minutes in cold saline and cut into 2-mm coronal slices with a rat brain matrix slicer. The slices were stained for 20 min at 37°C in a 2% solution of TTC in saline.

MRI Protocol

MRI diffusion imaging for mapping of the ADC was performed in 2 ways. During the hyperacute phase of the hemorrhage, a fast echo-planar imaging (EPI) diffusion sequence acquired alternating coronal diffusion and non–diffusion-weighted images in order to generate 60 ADC maps sequentially over a period of 12 min. SAH was induced 72 s (ie, 6 baseline ADC maps) after start of the echo-planar imaging series. Images of 3 slices were acquired every 2 s. To follow the evolution of diffusion changes over a longer time course, spin-echo DW images were then performed at 8 time points: before SAH, 30 minutes and 1 h after SAH, and then hourly for another 5 h (a total of 6 h). All DWI was performed on a 2-T GE Omega CSI spectrometer equipped with shielded gradients capable of producing±20 G/cm. The head of the rat was centered supinely in a 5.5-cm diameter birdcage radiofrequency coil.

EPI diffusion imaging parameters were as follows: 40 mm field of view, matrix size 64×64, TR=2 s, TE=50 ms, 1 average, 3 coronal slices, slice thickness=2 mm, and interslice gap=0.2 mm. The diffusion-sensitizing gradients were applied along the *Z* direction (ie, nose-tail). The ADC maps from the dynamic EPI scans were generated with a 12-s time resolution from a sequence of 6 images with the *b* values 0, 1300, 1300, 0, 1300, 1300 s/mm.^{2} Two sets of the 0, 1300, 1300 s/mm^2 images were used to improve the calculation of the ADC at the expense of temporal resolution.

The diffusion-weighted images for the higher resolution spin-echo imaging sequence were acquired with use of isotropic weighting methods to remove the confounding effects of anisotropic water diffusion on DW image intensity.[14] The isotropic weighting was achieved within a single scan by using diffusion-sensitizing gradient waveforms[15] that satisfy the orthogonality requirements detailed by Wong et al.[16] Each set of diffusion-sensitizing gradients before and after the radiofrequency pulse had a duration of 25 ms and produced gradient *b* values of 1300, 600, and 20 s/mm.^{2} Pixel-by-pixel maps of the ADC of water were calculated from these 3 sets of images.[17] The high-resolution spin-echo diffusion images were acquired with a 128×128 matrix size, field-of-view of 50 mm, TR=2500 ms, TE=80 ms, 1 average, 8 coronal slices, slice thickness of 1.5 mm, an interslice gap of 0.2 mm, and an acquisition time of 5.5 min.

Image Analysis

Image analysis was carried out using the image processing software MRVision (MRVision Co). For the fast EPI acquisitions, the 6 ADC maps obtained before advancement of the suture were averaged. All following ADC maps were pixelwise normalized to this averaged control ADC map. Areas with an ADC below 85% of control values were highlighted on all normalized ADC maps. The areas with ADC values below 85% of the control ADC, as measured before SAH, were highlighted also on ADC maps from the SE-DWI. The highlighted regions were transferred to a standardized brain section drawing, using transparency techniques to achieve overlay images. Relative ADC values over time were measured from 2 regions of interest in the somatosensory cortex of both hemispheres. The time of onset of ADC changes in ipsilateral and contralateral hemispheres was defined as the time point at which the ADC declined to below 85% of its control value.

Data are given as mean±SEM unless stated otherwise. Statistical analysis between groups was performed by 1-way analysis of variance (ANOVA), followed by Student's paired *t* test. A *P* value <0.05 was accepted as significant.

Results

General Physiological Parameters

The Table summarizes the physiological parameters before and after SAH. Arterial blood gases and core temperature were in the normal range throughout the experiment and did not differ significantly between groups. Likewise, the MAP in control animals was stable throughout the experiment. SAH in nonheparinized animals caused a brief decline in MAP of approximately 15% but quickly stabilized at pre-SAH level for the rest of the experiment. One of the nonheparinized animals developed an ADC decline of the entire brain at 6 h, correlating with a decline in MAP to 70 mm Hg. The same pattern was observed in all heparinized animals. The development of an ADC decline throughout the brain correlated with a lowering of the MAP to approximately 70 mm Hg and indicated brain death. Some of these animals had a preceding period of elevated MAP before the decline took place.

Visual Inspection of Brains

None of the control animals had any evidence of subarachnoid hemorrhage postmortem. In contrast, all other animals

General Physiological Parameters

		Time After SAH		
	Control	30 min	1 h	2 h/2–6 h
Arterial blood pressure, mm Hg				
Control	103±5	101±7	103±3	103±5
Nonheparinized	109±8	107±6	105±13	105±6
Heparinized	105±7	103±21	91±28	72±8
Body temperature, °C				
Control	37.3±0.1	37.7±0.3	37.3±0.7	37.2±0.6
Nonheparinized	38.0±0.5	37.5±0.7	37.3±0.9	37.5±0.7
Heparinized	37.3±0.5	37.0±1.0	36.8±0.4	36.6±0.7
Arterial Po_2, mm Hg				
Control	124±11		113±16	136±32
Nonheparinized	112±19		115±9	122±22
Heparinized	113±23		105±10	130±20
Arterial Pco_2, mm Hg				
Control	34±6		40±3	38±6
Nonheparinized	42±9		37±7	38±5
Heparinized	43±10		41±4	39±10
Arterial pH, U				
Control	7.40±0.05		7.36±0.02	7.41±0.07
Nonheparinized	7.35±0.05		7.37±0.05	7.33±0.04
Heparinized	7.30±0.04		7.31±0.04	7.36±0.11

All values are mean±SD in control (n=3), nonheparinized (n=6), and heparinized rats (n=5). Control and nonheparinized rats were followed for 6 h and heparinized rats for 2 h after induction of SAH.

had extensive subarachnoid hemorrhage. In nonheparinized animals, clotted and unclotted blood was found around the circle of Willis, distributed equally between both sides. Blood was also found as a thin layer overlying the cortex, around the brain stem, and, in most animals, in the ventricles. Subarachnoid blood was similarly distributed in heparinized animals, but no blood clots were found.

Diffusion Changes During Hyperacute SAH (EPI)

Measured absolute ADC values before intervention were similar for all groups. Averaged ADC ($\times 10^{-3}$ mm^2/s) values in the cortex were 0.72±0.01, 0.76±0.01, and 0.75±0.02 in control, nonheparinized, and heparinized animals, respectively.

In control animals, no significant ADC changes were detected throughout the observation period of 12 min after the suture was briefly advanced to the MCA origin and then retracted (Figure 1A).

In all nonheparinized animals, a rapid ADC decline was observed, starting in the ipsilateral somatosensory cortex. This area of ADC decline increased quickly by spreading out over the ipsilateral cortex and basal ganglia. In 5 of 6 animals in this group, contralateral ADC changes were observed. The spatial pattern of the ADC decline is depicted in Figure 2. The ADC decline on the contralateral side started either in the somatosensory cortex, as on the ipsilateral side, or in the parietal cortex close to the midline. The lesion area, as defined by at least a 85% drop in ADC, was maximal at the end of the 12-min observation period but was smaller on the contralateral side. The rapid ADC decrease in the ipsilateral somatosensory cortex occurred 106±8 s after the suture was advanced for induction of SAH (Figure 1B). This change was typically preceded by a slight ADC decrease starting in the first minute after SAH and resulted in a drop to approximately 75% of control. Similar ADC changes on the contralateral side started with a delay of 66±15 s after the ADC decline in the ipsilateral cortex.

In heparinized animals, ADC changes occurred in a very similar spatial pattern as in nonheparinized animals, starting in the ipsilateral somatosensory cortex and then spreading out in a similar manner (Figure 3). In 4 of 5 animals, ADC changed on the contralateral side during this initial time period, in 3 animals starting close to the midline in the parietal cortex and in 1 animal in the somatosensory cortex. The characteristics of the onset of ipsilateral ADC changes in this group (113±6 s) were similar to those in the nonheparinized animals (Figure 1C). However, the onset of contralateral ADC changes, 189±19 s later than ipsilateral, was significantly delayed ($P=0.0024$) compared with the nonheparinized animals.

Diffusion Changes During the 6 Hours After SAH (SE)

Absolute ADC values ($\times 10^{-3}$ mm^2/s) in the cortex measured prior to hemorrhage were 0.71±0.09 and 0.71±0.01 in the control and SAH groups, respectively.

Figure 4 shows diffusion changes observed during the 6-h observation period in a nonheparinized animal, while Figure 5 summarizes the temporal and spatial pattern of ADC

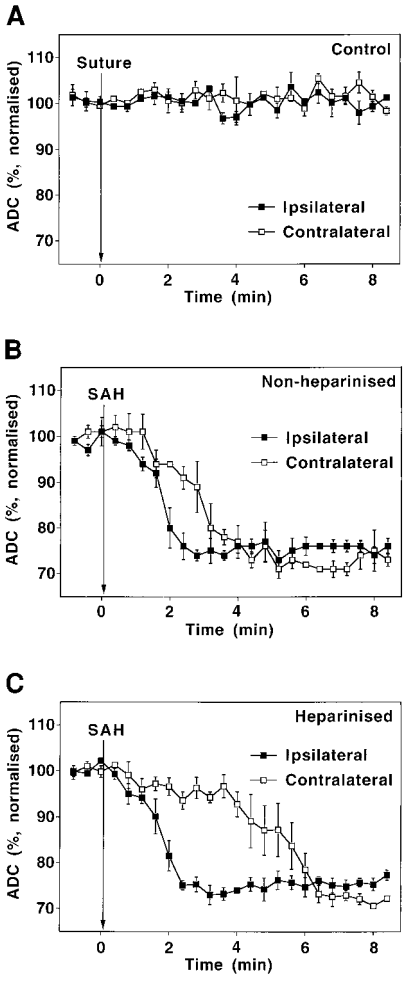

Figure 1. ADC changes during hyperacute SAH. ADC values are calculated from regions of interest in the somatosensory cortex of both hemispheres and normalized to the average of control values before advancement of the suture. ADC values (mean±SEM) are presented 1 min before and 8 min after suture advancement. Data points are given every 24 s. A, Brief advancement of the suture to the MCA origin without perforation of the circle of Willis did not induce any ADC changes in the control group. B, SAH in nonheparinized animals caused a rapid decline of ADC in the somatosensory cortex starting 106±8 s after SAH. The maximal reduction in ADC is to about 75% of normal. This decline was preceded by a gradual decrease of ADC within the first minute. ADC decreased in the corresponding region of the contralateral side, with a delay of 66±15 s in 4 animals of this group. C, SAH in heparinized animals started similar to that on the ipsilateral side, but with a significant longer delay of 189±19 s on the contralateral side, in 4 animals of this group.

changes seen in all of the 6 nonheparinized animals. The earliest ADC maps from SE-DWI images were obtained at 30 min after SAH, and the spatial distribution of ADC changes in these maps correlates well with those changes seen in the last ADC maps obtained from the EPI images (see Figures 2 and 5 for comparison). However, in the following hours, the area of ADC changes declined dramatically (Figures 4 to 6). In 1 animal, the ADC changes disappeared completely, and in another animal the area with ADC decline enlarged further to comprise the whole brain at 6 h. In 4 animals, the ADC lesion was confined to the ipsilateral somatosensory cortex at 6 h. In 4 of the heparinized animals, the ADC of the entire brain had

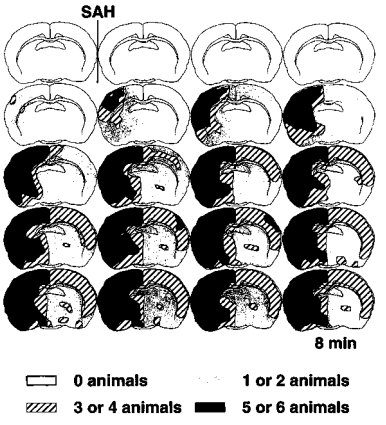

Figure 2. Spatial evolution of ADC changes during hyperacute SAH in nonheparinized animals. Areas with an ADC reduction of >85% were highlighted on ADC maps at the level of the bregma and transferred to standardized brain sections. Areas with an ADC decline in 5 or 6 animals are presented in black, in 3 or 4 animals with strips, and in 1 or 2 animals in gray. One section before and 19 sections after SAH are shown over a total time period of 8 min, with each section representing 24 s. The ADC declines began in the ipsilateral somatosensory cortex and spread within minutes over cortex and subcortical structures of this hemisphere. Delayed changes on the contralateral side started either in the corresponding somatosensory cortex or close to the midline in the parietal cortex and spread out over the hemisphere, but to a lesser spatial extent.

declined at 30 min after SAH (Figure 3), whereas in the fifth animal it had fully declined only at 2 h after SAH.

TTC Staining

Control animals showed completely normal staining of the brain after incubation in TTC solution. The white, unstained regions in the nonheparinized animals corresponded well with the areas of ADC changes (Figure 5).

Discussion

Our results establish that MR diffusion imaging is indeed capable of monitoring the impact of acute SAH in rat brain.

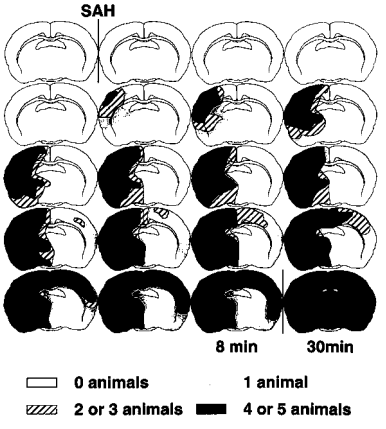

Figure 3. Spatial evolution of ADC changes during hyperacute SAH in heparinized animals. Results are presented as in Figure 2; the last section is replaced with a section representing the extent of ADC changes in SE-DWI at 30 min. ADC changes in this group evolved similar to that in nonheparinized animals, but changes on the contralateral side started significantly later. In addition, decline of the ADC in the whole brain at 30 min indicates brain death.

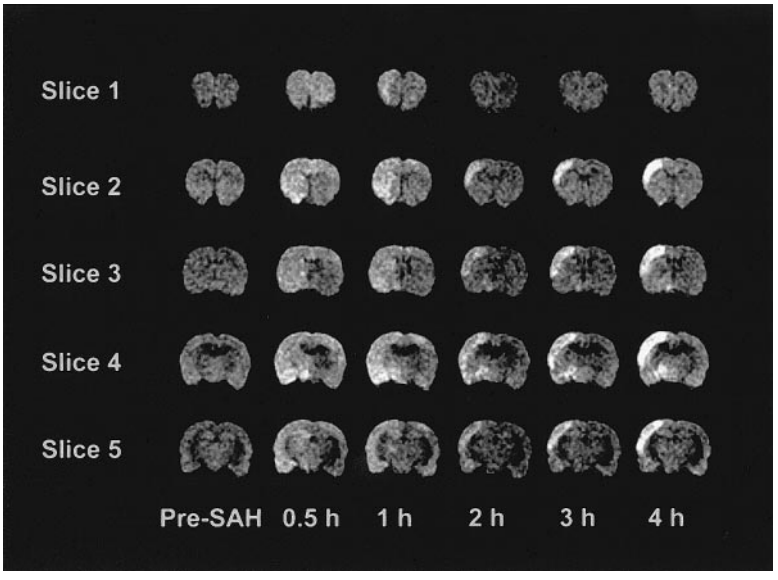

Figure 4. Diffusion-weighted imaging during acute SAH. Presented are 5 coronal slices through the central brain before and 5 time points after SAH. At 30 min after SAH, widespread hyperintensity is visible, comprising most of the ipsilateral hemisphere and the larger part of the contralateral cortex. Hyperintensity on DWI indicates a reduction of ADC. At 2 h after SAH, the hyperintense areas are dramatically reduced and are confined to the ipsilateral cortex. At 4 h after SAH, the hyperintense regions appear slightly enlarged again and brighter, indicating underlying changes in T2 signal intensity.

A sharp decline of ADC was consistently observed within 2 min after onset of SAH in the ipsilateral somatosensory cortex. From a localized initial region, the areas with reduced ADC spread within minutes over the ipsilateral hemisphere. In most animals, corresponding ADC reductions were seen on the contralateral side with a time delay of 1 min (nonheparinized rats) or 3 min (heparinized rats) relative to the ipsilateral side, either in the corresponding location to the ipsilateral cortex or in the parietal cortex close to the midline. The contralateral ADC changes spread out to a lesser extent than the ipsilateral side. The greater part of ADC changes in nonheparinized animals resolved within 2 h, whereas the ADC declined throughout the entire brain in heparinized animals as early as 30 min after SAH. A number of conclusions can be drawn from these observations.

Acute Vasospasm After SAH

The initial ADC reductions always occurred in the ipsilateral somatosensory cortex, in the most distal region supplied by the middle cerebral artery (MCA). This observation strongly suggests that the onset (but not the subsequent spreading; see below) of diffusion changes is related to vascular anatomy. Therefore, the occurrence of acute vasospasm can be hypothesized. The observation that the ADC changes on the contralateral side began either in the corresponding area or from a location close to the midline suggests that either the contralateral MCA or the anterior cerebral artery (ACA) develop vasospasm first.

The reduction of CBF due to decrease of CPP after SAH is well established.[4,5,18,19] Therefore, the initial ADC decrease in a circumscribed region of the ipsilateral somatosensory cortex most likely reflects critical ischemia caused by a combination of overall reduction of CBF and localized vasospasm.

The observation of delayed ADC decreases on the contralateral side provides evidence that it is not the perforation injury to a vessel itself which is causing vasospasm, although it might increase its severity and duration. It seems more likely that the presence of subarachnoid blood triggers the vasospasm and that the delay between the two hemispheres can be explained by the time the blood needs to reach the contralateral vessels in a comparable concentration to that on the ipsilateral side.

In this context it is interesting that a significant difference was observed in the time delay between the nonheparinized

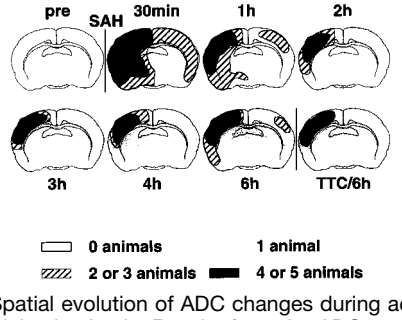

Figure 5. Spatial evolution of ADC changes during acute SAH in nonheparinized animals. Results from the ADC maps, as calculated from SE-DW images, are presented as in Figure 2 and the results from TTC staining of the matching brain sections are added for comparison at the end. The spatial extent of ADC changes is reduced after the 30-min time point.

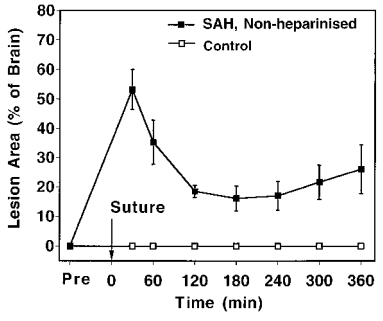

Figure 6. Spatial extent of ADC changes during acute SAH in control and nonheparinized animals. The brain area affected by a reduction in ADC below 85% of normal is expressed as a percentage of the whole brain area of a single coronal slice at the level of bregma (mean±SEM). The nonheparinized animal that developed an ADC decline of the whole brain was excluded from this analysis.

and heparinized animals for the diffusion changes to occur on the contralateral side: 66±15 s for nonheparinized animals compared with 189±19 s for heparinized animals. It would be expected that in heparinized animals the ICP would rise more quickly than in the nonheparinized animals, since the bleeding does not clot, and therefore the ADC would decline more rapidly. Instead, we found the opposite: ADC declines on the contralateral side started later in the heparinized animals. As the most likely explanation, heparin blocks the formation of thrombin, which is a strong vasoconstrictor.[20–22] This finding lets us conclude that thrombin plays a role, but not the only one, in acute vasospasm after SAH.

Our notion that acute vasospasm occurs after experimental SAH is in line with the results of a number of studies which have investigated the events immediately after the acute episode of SAH[4–6,18,23–26] and monitored CBF, ICP, and CPP. Although CPP was considerably decreased in these studies during a short time period after SAH, it returned to values close to normal after 15 to 20 min. One study reported a mismatch between CPP and CBF changes.[4] Another study observed differences between both hemispheres; the ipsilateral hemisphere to the hemorrhage had an earlier and more severe decrease of CBF and CBV than the contralateral hemisphere.[4,19] Interestingly, the CBF/CBV decrease was found to precede the increase in ICP. Another study has shown directly a biphasic response of vasospasm after SAH through use of angiographic methods, with the first vasospasm taking place immediately after the bleed and the second occurring days later, depending on the animal model.[7] Most of these studies conclude from their measurements that vasospasm plays a role during acute SAH. However, the occurrence of early vasospasm in humans is uncertain (for a review, see Jakobsen[8]), since it is very difficult to study. So far, only a few cases of acute vasospasm, when SAH occurred during cerebral angiography, have been reported.[27,28]

"Spreading Depolarization" of Brain Tissue After SAH

The spreading wavefront of diffusion changes always starts at a localized region and then crosses vascular territories as it spreads. It is therefore unlikely that the spreading of diffusion changes reflects ischemic changes due to decrease of cerebral perfusion pressure or vasospasm only. In the first case, changes would have to be expected to start throughout the brain; in the second case, they would be confined to vascular territories. The spatial and temporal pattern of diffusion changes observed in our study indicates the occurrence of "spreading depolarization" of brain tissue, in analogy to spreading depression. Spreading depression and the related MR diffusion changes last for only 1 to 2 min,[29,30] whereas the changes observed in this study persisted much longer.

The greater part of the widespread diffusion changes, which evolved during the initial 8 min after SAH, resolved within the first 2 h in nonheparinized animals. The dynamic of diffusion changes observed in this study certainly is remarkable (Figures 2, 4, and 5), but early resolution of DWI changes for a variety of reasons has been described by other authors as well.[31–34] In our study, the resolution of DWI changes can be interpreted as delayed repolarization after spreading depolarization of brain tissue. Repolarization is an energy-demanding process and therefore depends on sufficient blood supply.[35] It has been shown previously that the duration of spreading depression depends on the level of oligemia of the tissue.[12] It is likely that CBF immediately after SAH is reduced to such a level that repolarization of brain tissue is delayed. However, only a small cortical region, centered around the area where the very first changes occurred, remained abnormal on ADC maps (Figure 5) and did not stain in TTC solution at 6 h.

DWI Changes Reflect Severity of SAH

The comparison between nonheparinized and heparinized animals clearly shows that time course and spatial extent of ADC changes reflect severity of SAH. In heparinized animals, which can be expected to have a persistent hemorrhage and therefore a continuous drop of CPP, the resulting ischemia is characterized by a lack of recovery and a drop of ADC throughout the brain. In nonheparinized animals, recovery of ADC changes reflect stabilization of CBF on levels above the critical threshold for infarction. However, persistent ADC changes in circumscribed regions at 2 h after SAH resulted in demarcated areas on TTC staining at 6 h. Therefore, early DWI might have a predictive value for recovery of brain tissue after SAH and therefore could help in clinical decision making. More speculative, DWI might be useful in monitoring delayed cerebral ischemia after SAH in patients, because ADC decreases are to be expected before changes in cerebral CT if CBF drops below an ischemic threshold.[9]

In conclusion, MR diffusion imaging yields new insight into the acute pathophysiology of SAH and is capable of monitoring the initial impact of acute SAH on the brain. The reduced ADC values reflect cellular depolarization of brain tissue after SAH. The relation of the initial diffusion changes to vascular territories suggests a role for acute vasospasm. The spatial-temporal pattern of the spreading of diffusion changes indicates the occurrence of "spreading depolarization" of brain tissue. In addition, DWI of heparinized animals with more severe hemorrhage demonstrates that time course and spatial extent of reductions in ADC reflect the severity of SAH.

Acknowledgments

Support from the Alexander von Humboldt-Stiftung (Dr Busch), Alberta Heritage Foundation for Medical Research (Dr Beaulieu), the Lucas Foundation, and the Phil N. Allen Trust is gratefully acknowledged. We thank Maj Hedehus, PhD, and Kim Butts, PhD, for the isotropic diffusion pulse sequence and David Kunis for help with the documentation.

References

1. Vermeulen M. Subarachnoid haemorrhage: diagnosis and treatment. *J Neurol*. 1996;243:496–501.
2. van Gijn J. Subarachnoid haemorrhage. *Lancet*. 1992;339:653–655.
3. Broderick JP, Brott TG, Duldner JE, Tomsick T, Leach A. Initial and recurrent bleeding are the major causes of death following subarachnoid hemorrhage. *Stroke*. 1994;25:1342–1347.
4. Bederson JB, Germano IM, Guarino L. Cortical blood flow and cerebral perfusion pressure in a new noncraniotomy model of subarachnoid hemorrhage in the rat. *Stroke*. 1995;26:1086–1091.
5. Veelken JA, Laing RJ, Jakubowski J. The Sheffield model of subarachnoid hemorrhage in rats. *Stroke*. 1995;26:1279–1283.
6. Bederson JB, Levy AL, Ding WH, Kahn R, DiPerna CA, Jenkins AL, Vallabhajosyula P. Acute vasoconstriction after subarachnoid hemorrhage. *Neurosurgery*. 1998;42:352–360.

7. Symon L. An experimental study of traumatic cerebral vascular spasm. *J Neurol Neurosurg Psychiatry*. 1967;30:497–505.
8. Jakobsen M. Role of initial brain ischemia in subarachnoid hemorrhage following aneurysm rupture: a pathophysiological survey. *Acta Neurol Scand Suppl*. 1992;141:1–33.
9. Moseley ME, Cohen Y, Mintorovitch J, Chileuitt L, Shimizu H, Kucharczyk J, Wendland MF, Weinstein PR. Early detection of regional cerebral ischemia in cats: comparison of diffusion- and T2-weighted MRI and spectroscopy. *Magn Reson Med*. 1990;14:330–346.
10. Warach S, Chien D, Li W, Ronthal M, Edelman RR. Fast magnetic resonance diffusion-weighted imaging of acute human stroke. *Neurology*. 1992;42:1717–1723.
11. Pierpaoli C, Alger JR, Righini A, Mattiello J, Dickerson R, Des Pres D, Barnett A, Di Chiro G. High temporal resolution diffusion MRI of global cerebral ischemia and reperfusion. *J Cereb Blood Flow Metab*. 1996;16: 892–905.
12. Rother J, de Crespigny A, D'Arceuil H, Iwai K, Moseley ME. Recovery of apparent diffusion coefficient after ischemia-induced spreading depression relates to cerebral perfusion gradient. *Stroke*. 1996;27: 980–986.
13. Kohno K, Back T, Hoehn-Berlage M, Hossmann KA. A modified rat model of middle cerebral artery thread occlusion under electrophysiological control for magnetic resonance investigations. *Magn Reson Imaging*. 1995;13:65–71.
14. van Gelderen P, de Vleeschouwer MH, Des Pres D, Pekar J, van Zijl PC, Moonen CT. Water diffusion and acute stroke. *Magn Reson Med*. 1994; 31:154–163.
15. Butts K, Pauly J, de Crespigny A, Moseley M. Isotropic diffusion-weighted and spiral-navigated interleaved EPI for routine imaging of acute stroke. *Magn Reson Med*. 1997;38:741–749.
16. Wong EC, Cox RW, Song AW. Optimized isotropic diffusion weighting. *Magn Reson Med*. 1995;34:139–143.
17. Le Bihan D. Molecular diffusion, tissue microdynamics and microstructure. *NMR Biomed*. 1995;8:375–386.
18. Jakubowski J, Bell BA, Symon L, Zawirski MB, Francis DM. A primate model of subarachnoid hemorrhage: change in regional cerebral blood flow, autoregulation carbon dioxide reactivity, and central conduction time. *Stroke*. 1982;13:601–611.
19. Kuyama H, Ladds A, Branston NM, Nitta M, Symon L. An experimental study of acute subarachnoid haemorrhage in baboons: changes in cerebral blood volume, blood flow, electrical activity and water content. *J Neurol Neurosurg Psychiatry*. 1984;47:354–364.
20. Chimowitz MI, and Pessin MS. Is there a role for heparin in the management of complications of subarachnoid hemorrhage? *Stroke*. 1987;18: 1169–1172.
21. Haver VM, and Namm DH. Generation of a vasoactive substance in human plasma during coagulation: evidence of thrombin-induced contraction of rabbit aorta and dog coronary artery. *Blood Vessels*. 1983;20: 92–98.
22. White RP. Comparison of the inhibitory effects of antithrombin III, alpha 2-macroglobulin, and thrombin in human basilar arteries: relevance to cerebral vasospasm. *J Cereb Blood Flow Metab*. 1987;7:68–73.
23. Delgado TJ, Brismar J, Svendgaard NA. Subarachnoid haemorrhage in the rat: angiography and fluorescence microscopy of the major cerebral arteries. *Stroke*. 1985;16:595–602.
24. Jackowski A, Crockard A, Burnstock G, Russell RR, Kristek F. The time course of intracranial pathophysiological changes following experimental subarachnoid haemorrhage in the rat. *J Cereb Blood Flow Metab*. 1990; 10:835–849.
25. McCormick PW, McCormick J, Zabramski JM, Spetzler RF. Hemodynamics of subarachnoid hemorrhage arrest. *J Neurosurg*. 1994;80: 710–715.
26. Svendgaard NA, Brismar J, Delgado TJ, Rosengren E. Subarachnoid haemorrhage in the rat: effect on the development of vasospasm of selective lesions of the catecholamine systems in the lower brain stem. *Stroke*. 1985;16:602–608.
27. Taneda M, Otsuki H, Kumura E, Sakaguchi T. Angiographic demonstration of acute phase of intracranial arterial spasm following aneurysm rupture. Case report. *J Neurosurg*. 1990;73:958–961.
28. Wilkins RH. Aneurysm rupture during angiography: does acute vasospasm occur? *Surg Neurol*. 1976;5:299–303.
29. Hansen AJ, Quistorff B, Gjedde A. Relationship between local changes in cortical blood flow and extracellular K+ during spreading depression. *Acta Physiol Scand*. 1980;109:1–6.
30. Latour LL, Hasegawa Y, Formato JE, Fisher M, Sotak CH. Spreading waves of decreased diffusion coefficient after cortical stimulation in the rat brain. *Magn Reson Med*. 1994;32:189–198.
31. Busch E, Hoehn-Berlage M, Eis M, Gyngell ML, Hossmann KA. Simultaneous recording of EEG, DC potential and diffusion-weighted NMR imaging during potassium induced cortical spreading depression in rats. *NMR Biomed*. 1995;8:59–64.
32. Minematsu K, Li L, Sotak CH, Davis MA, Fisher M. Reversible focal ischemic injury demonstrated by diffusion-weighted magnetic resonance imaging in rats. *Stroke*. 1992;23:1304–1310.
33. Fischer M, Bockhorst K, Hoehn-Berlage M, Schmitz B, Hossmann KA. Imaging of the apparent diffusion coefficient for the evaluation of cerebral metabolic recovery after cardiac arrest. *Magn Reson Imaging*. 1995;13:781–790.
34. Zhong J, Petroff OA, Prichard JW, Gore JC. Changes in water diffusion and relaxation properties of rat cerebrum during status epilepticus. *Magn Reson Med*. 1993;30:241–246.
35. Mies G, and Paschen W. Regional changes of blood flow, glucose, and ATP content determined on brain sections during a single passage of spreading depression in rat brain cortex. *Exp. Neurol*. 1984;84:249–258.

Editorial Comment

There is no doubt that application of newer MRI techniques will further advance our knowledge and insight into the pathophysiology of many diseases, including subarachnoid hemorrhage (SAH) in experimental animals and humans. Although somewhat speculative, the authors' conclusion that in rats SAH effects its changes through a combination of decreased cerebral perfusion pressure (CPP) and vasospasm is reasonable. This is a descriptive study, lacking a clearly stated hypothesis, so it is possible that the authors were caught off-guard themselves. Had they expected these findings and hypothesized their explanation in advance, they probably would have added intracranial pressure measurements to the experiments. A finding of decreased CPP in the heparinized animals compared with the nonheparinized group, and the measured extent of this difference, would have bolstered their case.

I do not share the authors' view that these techniques, elegant as they may be, should be applied to patients with SAH soon. As it stands now and in the foreseeable future, there is nothing we can do about the acute effects of aneurysmal rupture, even in the setting of the intensive care or during angiography. This is not to say, however, that experiments as described here are not important. Every little piece falling in place in the giant jigsaw puzzle that is SAH will eventually lead to more effective overall treatment.

J. Paul Muizelaar, MD, PhD, *Guest Editor*
Department of Neurosurgery
University of California, Davis
Sacramento, California